Hydrolysis Mechanisms for the Acetylpyridinephenylhydrazone Ligand in Sulfuric Acid

Begoña García,* María S. Muñoz, Saturnino Ibeas, and José M. Leal

Universidad de Burgos, Departamento de Química, Laboratorio de Química Física, 09001 Burgos, Spain

Received January 21, 2000

The excess acidity method was applied to rate data obtained for 2-acetylpyridinephenylhydrazone hydrolysis in strong acid media using various aqueous/organic solvents, and it was observed that the reaction rate decreases with increasing permittivity of the medium. Two hydrolysis mechanisms are indicated. Below 0.6 M H_2SO_4, no hydrolysis was observed; between 0.6 and 6.0 M H_2SO_4, the substrate hydrolyzes by an A-S_E2 mechanism and switches to an A-2 mechanism at higher acidity. This change of mechanism was justified on the basis of the syn and anti rotational conformers of the diene $-N_{(1)}=C-C=N_{(2)}-$ group; the greater stability of the former can be explained by the formation of hydrogen bonds between the proton and the $N_{(1)}$ and $N_{(2)}$ nitrogen atoms, giving rise to a very stable five-membered ring. If the syn conformer is predominant, then no hydrolysis is observed; above 0.6 M, the attack of a second proton gives rise to a balance between the syn and anti forms, the latter being responsible for the hydrolysis of the hydrazone group.

Introduction

Cyclometalated complexes constitute an important tool to activate the C−H bond, forming transition-metal complexes the structures of which have often been suggested as intermediate species in many metal-catalyzed chemical reactions.[1] In particular, cyclopalladated complexes possess a highly reactive metal−carbon σ bond, which becomes stabilized by further coordination to metal of a donor heteroatom; these compounds manifest quite a rich chemistry, of growing interest among scientists after the contributions by Cope et al.[2] and Dunina et al.[3] Processes such as conversion and storing of solar energy can actually be interpreted on the basis of the photochemical activity of these coordination complexes, a number of which exhibit remarkable biochemical activity and liquid crystal properties[4,5] and can be used to introduce heavy metal and fluorescent markers in proteins and polypeptides.[6]

In a previous paper, we reported on the deprotonation in basic medium of five orthometalated complexes, structurally based on 2-acetylpyridinephenylhydrazones coordinated to Pd(II), to which different radicals can be attached;[7] they contain some basic nitrogen atoms, and therefore, they are susceptible to protonation. However, in acidic medium, these complexes undergo chemical reactions with not yet well-known mechanisms. In an attempt to delineate such mechanisms, we studied the hydrolysis of the ligand 2-acetylpyridinephenylhydrazone, the structure of which is shown in the Schemes 1 and 2; in this work, we report on the different kinetic behavior observed depending on the medium acidity. At low acidities, no hydrolysis was observed; however, at intermediate acidities (between 0.6 and 6.0 M H_2SO_4), the reaction proceeds by rate-determining proton attack to the imine nitrogen (A-S_E2 mechanism). At higher acidities (between 6.5 and 11.8 M H_2SO_4), the reaction proceeds by nucleophilic attack of a water molecule on the protonated substrate (A-2 mechanism). Given that the ligand has three basic nitrogen atoms, the acidities of the proton-transfer sites needed to establish the reaction mechanisms were also determined.

Scheme 1. AS_E-2 Mechanism

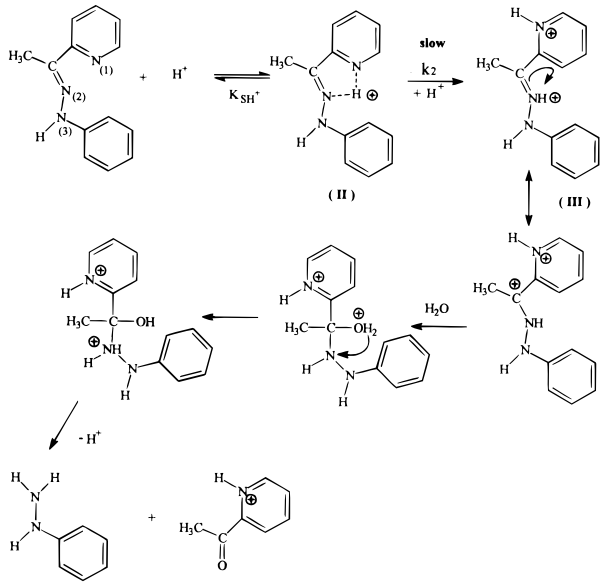

Experimental Section

The ligand 2-acetylpyridinephenylhydrazone was synthesized as described elsewhere;[8] the other reagents were commercially available. The spectral curves were recorded on a

(1) Crabtree, R. H. *Chem. Rev.* **1985**, *85*, 245.
(2) Cope, C. A.; Friederich, E. C. J. *J. Am. Chem. Soc.* **1968**, *90*, 909.
(3) Dunina, V. V.; Zalevskaya, O. A.; Potapop, V. M. *Usp. Khim.* **1988**, *57*, 434.
(4) Newkome, G. R.; Puckett, W. Q. E.; Kiefer G. E. *Inorg. Chem.* **1985**, *24*, 811.
(5) Halpern, J. *Inorg. Chim. Acta* **1985**, *41*, 100.
(6) Sokolov, V. I.; Nechaeva, K. S.; Reutov, O. A. *Zh. Org. Khim.* **1983**, *19*, 1103.
(7) Diez-Izarra, J. L.; García, B.; Ibeas, S.; Leal, J. M.; García-Herbosa, G.; Muñoz, A. *React. Funct. Polym.* **1998**, *36*, 227.
(8) Espinet, P.; García, G.; Herrero, F. J.; Jeannin, Y.; Philoche-Levisalles, M. *Inorg. Chem.* **1989**, *28*, 4207.

10.1021/jo000085m CCC: $19.00
Published on Web 05/18/2000

Scheme 2. A-2 Mechanism

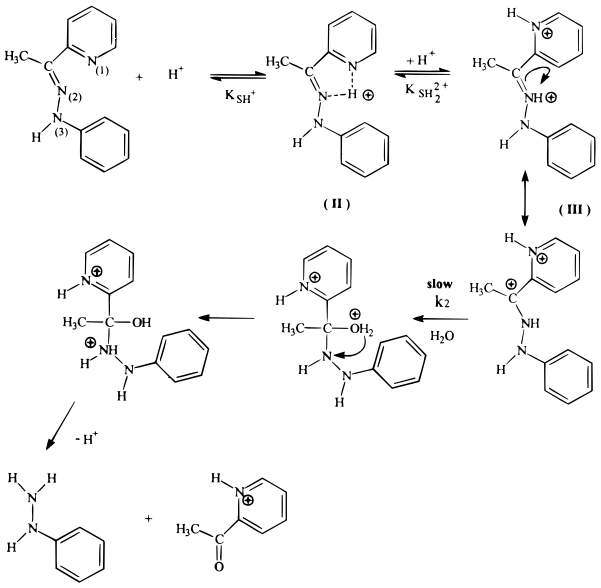

HP8452A spectrophotometer with a diode array detection system and equipped with a temperature cell-holder adapter electrically regulated and controlled by computer. The pH readings were taken with a pHM92 Lab Radiometer pH-meter (±0.01 units). Since the substrate is only sparingly soluble in pure water, to determine the solvent effect on the kinetics the experiments were carried out using different aqueous/organic solvents, containing dimethyl sulfoxide (DMSO) and ethanol (EtOH), in the following percentages: 10% v/v DMSO/H_2O, 30% v/v EtOH/H_2O, and 50% v/v EtOH/H_2O. Sulfuric acid was used to attain the required acidity in the medium. Sulfuric acid solutions were prepared by careful addition of the appropriate amounts of commercial H_2SO_4 to a 100 mL bottle containing a known amount of doubly distilled deionized water, the resulting acidity being determined by titration. Solutions of the substrate in 30% v/v EtOH/H_2O mixtures were always freshly prepared directly in the quartz cell by syringing 0.30 mL of pure ethanol to 1.4 mL of the adequate H_2SO_4 solution; after reaching thermal equilibrium, 0.30 mL of the proper sample of the substrate dissolved in pure ethanol (6.67×10^{-4} M) was added to the cell. A similar procedure was used with the other solvents.

The pH readings were measured directly with a glass electrode, which was calibrated in an aqueous medium. However, the measurable pH(R) readings differed by a δ quantity from the value measured using the buffer corresponding to the system in pure water.[9] Thus, due to the aqueous/organic mixtures used as solvents, it was necessary to correct the pH values using the equation $pH^* = pH(R) - \delta$; the δ parameter was essentially constant for a given aqueous/organic mixture at constant temperature; its amount was negligible for 10% DMSO−H_2O and tends to 0.085 and 0.16 for 30% and 50% EtOH/H_2O, respectively. Outside the pH range, the proton concentration C_{H^+} for each H_2SO_4 concentration was taken from literature sources.[10] The Lambert−Beer law was assessed at all wavelengths used.

The kinetic study was carried out by monitoring the decrease with time of the substrate absorbance reading, measured at the maximum wavelength. In all cases, the reaction was followed at least up to 90%, which corresponds to a reaction time larger than 3.32 ln $2/k_{obs}$, k_{obs} being the observed rate constant.[11] Within the acidity range investigated, no dependence of the rate constant on the substrate concentration was observed. In all experiments the working temperature was 25 °C. All kinetic runs were performed in duplicate.

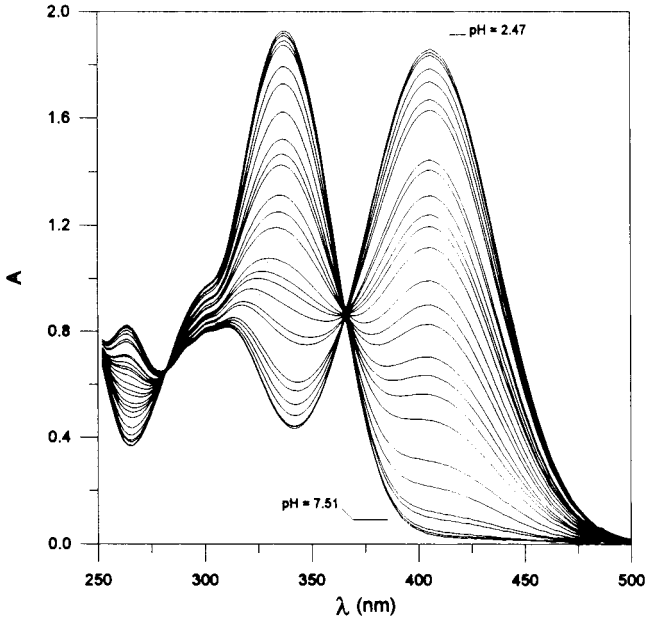

Figure 1. UV−vis absorption spectral curves of a 10^{-4} M 2-acetyl-pyridinephenylhydrazone solution in 10% DMSO/H_2O. $T = 25$ °C.

Table 1. pK_{SH}^+ Values as a Function of Solvent Permittivity, ϵ, and Wavelengths of Maximum Absorption, λ_{max}

solvent	pK_{SH}^+	ϵ	λ_{max} (nm)
10% DMSO/H_2O	4.9	78.0[49]	404
30% EtOH/H_2O	4.7	64.4[50]	408
50% EtOH/H_2O	4.4	53.4[50]	412

Results and Discussion

Figure 1 shows the set of spectral curves of a 10^{-4} M substrate solution, recorded upon variation of medium acidity in 10% DMSO/H_2O mixture; sets similar to this were recorded with the other mixed solvents. The procedure used to calculate pK_{SH}^+ values based on UV−vis spectroscopic measurements was previously described;[12,13] the values are listed in Table 1 along with the solvent permittivity, ϵ, and the wavelength of maximum absorption. In view of the basic character of the N atoms of the ligand, and given the dissociation constant of pyridinium ion, $pK_{SH}^+ = 5.2$, it is reasonable to ascribe these constants to $N_{(1)}$-protonation of the pyridine moiety;[14] on the other hand, given that the structure of 2-acetyl-pyridinephenylhydrazone was shown to be planar,[8] the proton entering in the "pyridine" $N_{(1)}$ atom becomes hydrogen-bonded to the "imine" $N_{(2)}$ nitrogen atom, forming a stable five-membered ring that establishes the syn structure (II) (Schemes 1 and 2) of the diene group. No hydrolysis was observed with this conformer. The pK_{SH}^+ values decreased as the solvent permittivity decreased; these variations in pK_{SH}^+ were ascribed to medium effects, these being defined as the ratio between

(9) Perrin, D. D.; Dempsey, B. *Buffers for pH and Metal Ion Control*; Chapman and Hall: New York, 1979; pp 77−93.
(10) Cox, R. A.; Yates, K. *J. Am. Chem. Soc.* **1978**, *100*, 3861.
(11) Espenson J. H. *Chemical Kinetics and Reactions Mechanims*; 2nd ed.; McGraw-Hill: New York, 1995.
(12) García, B.; Leal, J. M. *Collect. Czech. Chem. Commun.* **1987**, *52*, 1087.
(13) García, B.; Palacios, J. C. *Ber. Bunsen-Ges. Phys. Chem.* **1988**, *92*, 696.
(14) Pine, S. H.; Hendrickson, J. B.; Cram, D. J.; Hammond, G. S. In *Química Orgánica*, 2nd ed.; McGraw-Hill: Mexico D.F., 1993.

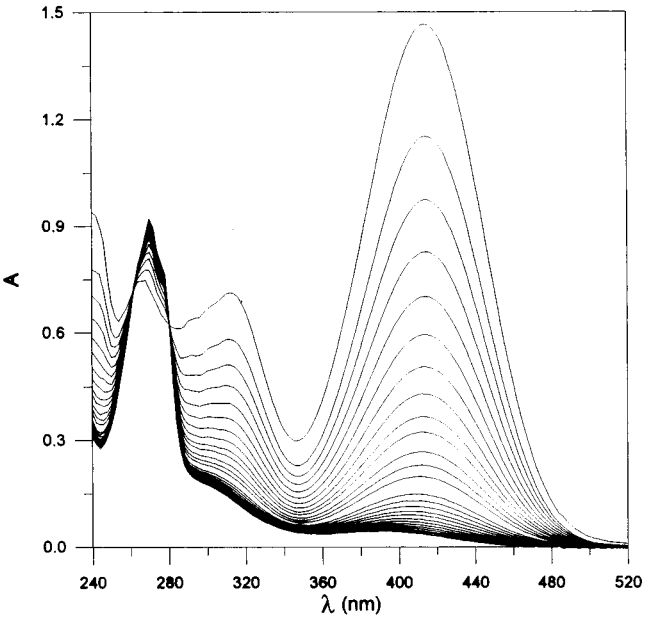

Figure 2. Absorption UV−vis spectral curves corresponding to hydrolysis of 2-acetylpyridinephenylhydrazone in 10.37 M H_2SO_4; time interval, 400 s.

the proton's activity coefficients in the solvent used and in water.[15] As already reported,[16] a bathochromic shift was also observed as the solvent polarity decreases.

However, in more highly acidic media a decrease in the substrate peak due to hydrolysis was observed; the observed rate constants, k_{obs}, were calculated by nonlinear least-squares regression,[17] using eq 1,

$$A = A_\infty - (A_o - A_\infty)e^{-k_{obs}t} \quad (1)$$

where A_o and A_∞ stand for the initial and final absorbance readings and A those at different reaction times, respectively. The initial values introduced to calculate these parameters are A_o, the first reading, and $A_\infty = 1.25^*$ (last absorbance measured) $- 0.25A_o$, $k_{obs} = 2/$(total reaction time). This procedure has the advantage that the absorbance readings need not to be taken at constant time intervals, nor is it necessary to monitor the reaction to completion.[17] The computer program used for the fitting of data is based on the Macquart−Lavengur method; after introducing the initial estimated values, the process is iterated until convergence is achieved for the minimum value of the χ^2 parameter.

As an example, Figure 2 shows the spectral curves recorded at different time intervals. Table 2 summarizes the k_{obs} values determined at different acidity levels for each of the different aqueous/organic solvents used. Figure 3 shows the change of k_{obs} with H_2SO_4 concentration using three different mixed solvents; the profiles of the three plots are similar and exhibit two stretches with different slopes; in the first stretch (0.6−6.0 M), k_{obs} increased with an increase in acidity only very slowly compared to the sharp increase observed above 6.0 M H_2SO_4, this feature reflecting that another mechanism is taking over at higher acidity.

To determine the reaction mechanism at medium and high acidity levels, available methods of dealing with kinetic data such as those of Zucker−Hammett,[18] Bunnett,[19] LFER,[20] and Cox−Yates[21,22] can be used. The three first treatments have the advantage of introducing the acid concentration in terms of the Hammett acidity function, H_o;[23] however, as H_o was originally defined using aniline as the reference base, which is structurally very distinct from the substrate used here, the excess acidity method proposed by Cox−Yates was preferred, yielding consistent results. The excess acidity, which represents the extra acidity of the medium due to its nonideal behavior, manifests the very useful property of being 0 in the standard state of activity coefficients unity and has become a powerful tool to study the effect of medium acidity upon the rate and equilibrium of a reaction, thus enabling us distinguish between three hydrolysis mechanisms:[24]

(i) A-1 Mechanism. If the starting material is SH^+, the substrate predominantly protonated under the reaction conditions, then the following mechanism applies:

$$SH^+ + H^+ \overset{K_{SH_2^{2+}}}{\rightleftharpoons} SH_2^{2+} \text{ fast} \quad (2)$$

$$SH_2^{2+} \xrightarrow{k_1} A^{2+} \text{ slow} \quad (3)$$

$$A^{2+} + H_2O \rightarrow P \text{ fast} \quad (4)$$

involving a fast preequilibrium protonation of SH^+, followed by rate-determining unimolecular reaction of SH_2^{2+} either to some intermediate species A^{2+}, which subsequently reacts quickly, or directly to products. The relevant rate equation is

$$\log k_{obs} - \log \frac{C_{SH^+}}{C_{SH_2^{2+}} + C_{SH^+}} - \log C_{H^+} = \log \frac{k_1}{K_{SH_2^{2+}}} + m^\ddagger m^* X \quad (5)$$

where the slope parameter $m^\ddagger$ measures the position of the transition state and correlates the activity coefficients of the substrate with those of the transition state, eq 6; the m^* parameter, defined in eq 7, relates the activity coefficients of the substrate and those of the standard base used as a reference in the definition of X:

$$\log \frac{f_{SH^+} f_{H^+}}{f_\ddagger} = m^\ddagger \log \frac{f_{SH^+} f_{H^+}}{f_{SH_2^{2+}}} = m^\ddagger m^* X \quad (6)$$

$$\log \frac{f_{SH^+} f_{H^+}}{f_{SH_2^{2+}}} = \log \frac{f_B f_{H^+}}{f_{BH^+}} = m^* X \quad (7)$$

To find out the $m^\ddagger$ value and therefore to be able to establish the reaction mechanism, the proper value for m^* corresponding to protonation equilibrium in high acidity, $pK_{SH_2^{2+}}$, must also be determined. The plot of the left-hand side of eq 5 vs X should give a straight line,

(15) Bates, R. G. *Determination of pH. Theory and Practice*; John Wiley & Sons: New York, 1973.
(16) Zhou, J. W.; Li, Y. T.; Tang, Y. W.; Song, X. Q. *J. Solution Chem.* **1995**, *24*, 625.
(17) Moore, P. *J. Chem. Soc., Faraday Trans. 1* **1972**, *68*, 1890.
(18) Zucker, L.; Hammett, L. P. *J. Am. Chem. Soc.* **1939**, *61*, 2791.
(19) Bunnett, J. F. *J. Am. Chem. Soc.* **1961**, *83*, 4956.
(20) Bunnett, J. F.; Olsen F. P. *Chem. Commun.* **1965**, 601; *Can. J. Chem.* **1966**, *44*, 1899.
(21) Cox, R. A. *Acc. Chem. Res.* **1987**, *20*, 27.
(22) Cox, R. A. *Adv. Phys. Org. Chem.* **2000**, in press.
(23) Hammett, L. P.; Deyrup, A. J. *J. Am. Chem. Soc.* **1932**, *54*, 2721.
(24) Cox, R. A.; Yates, K. *Can. J. Chem.* **1981**, *59*, 1560.

Table 2. Values of the k_{Obs} Rate Constants in H_2SO_4 at 25 °C

10% DMSO/H_2O		30% EtOH/H_2O		50% EtOH/H_2O	
$[H_2SO_4]$ (M)	$k_{obs} \times 10^5$ (s^{-1})	$[H_2SO_4]$ (M)	$k_{obs} \times 10^5$ (s^{-1})	$[H_2SO_4]$ (M)	$k_{obs} \times 10^5$ (s^{-1})
0.65	0.342 ± 0.001	3.03	0.771 ± 0.001	3.24	0.481 ± 0.001
1.30	0.691 ± 0.004	4.03	1.218 ± 0.001	3.96	0.662 ± 0.002
1.95	1.014 ± 0.001	4.54	1.582 ± 0.005	4.32	0.789 ± 0.003
2.59	1.399 ± 0.001	5.04	2.157 ± 0.002	4.68	0.953± 0.002
3.24	2.022 ± 0.002	5.55	2.897 ± 0.002	5.04	1.089 ± 0.002
3.89	2.724 ± 0.003	6.05	3.935 ± 0.007	5.22	1.344 ± 0.003
4.54	3.338 ± 0.002	6.56	5.706 ± 0.009	5.40	1.599 ± 0.001
5.19	4.304 ± 0.003	7.31	8.60 ± 0.02	5.58	1.929 ± 0.003
5.84	5.816 ± 0.002	7.56	11.34 ± 0.02	5.76	1.994 ± 0.002
6.48	8.261 ± 0.005	7.82	12.46 ± 0.02	5.94	2.443 ± 0.003
7.13	11.27 ± 0.01	8.07	15.47 ± 0.05	6.12	2.977± 0.003
7.78	15.55 ± 0.01	8.32	17.89 ± 0.01	6.30	3.435 ± 0.007
8.43	22.01 ± 0.02	8.57	20.49 ± 0.01	6.48	3.571 ± 0.006
9.08	29.03 ± 0.02	8.83	24.20 ± 0.01	6.66	4.518 ± 0.004
9.40	35.36 ± 0.02	9.33	30.47 ± 0.03	6.84	5.203 ± 0.006
9.72	44.00 ± 0.07	9.58	34.54 ± 0.06	7.02	6.109 ± 0.009
10.05	53.2 ± 0.2	9.83	37.65 ± 0.08	7.20	6.595 ± 0.009
10.37	57.8 ± 0.2	10.09	40.6 ± 0.1	7.38	7.51 ± 0.01
10.70	69.2 ± 0.4	10.34	44.2 ± 0.3	7.56	8.54 ± 0.01
11.02	72.5 ± 0.3			7.92	10.12 ± 0.03
11.35	82.1 ± 0.6			8.29	10.64 ± 0.04
11.67	82.4 ± 0.8			8.65	12.01 ± 0.03
				9.01	13.93 ± 0.07

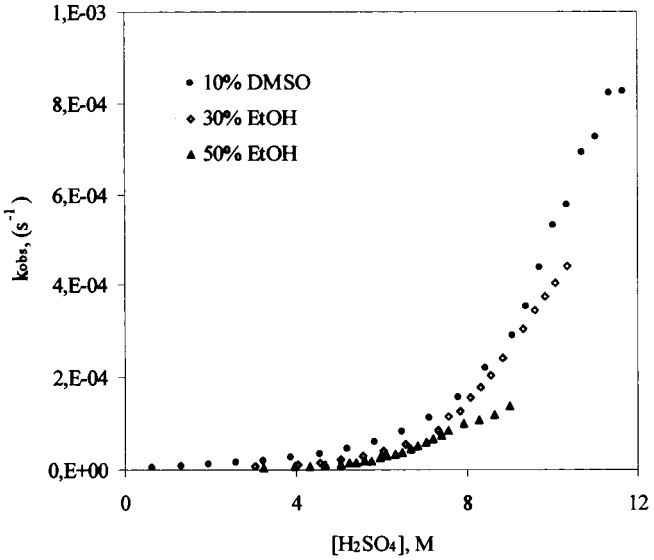

Figure 3. log k_{obs} vs $[H_2SO_4]$ profile for 2-acetylpyridine-phenylhydrazone at 25 °C using three different mixed solvents.

the ordinate of which provides $\log(k_1/K_{SH_2^{2+}})$; in addition, the $m^{\ddagger}$ value is greater than 1 and normally falls between 2 and 3. This treatment was applied to determine the mechanism of a variety of hydrolyses, including a number of esters, substituted benzaldehydes, and other substrates,[25−29] as well as the chromic acid oxidation of propanal[30] and glycolic acid.[31]

(ii) A-2 Mechanism. This is like the A-1 mechanism except that the diprotonated substrate, instead of reacting alone, reacts with an additional species in the rate-determining transition state

$$SH^+ + H^+ \overset{K_{SH_2^{2+}}}{\rightleftharpoons} SH_2^{2+} \text{ fast} \quad (2)$$

$$SH_2^{2+} + n\text{Nu} \xrightarrow{k_2} P \text{ slow} \quad (8)$$

where Nu stands for the nucleophile (normally water) and n is the number of molecules. The relevant rate equation derived for this mechanism is as follows

$$\log k_{obs} - \log \frac{C_{SH^+}}{C_{SH_2^{2+}} + C_{SH^+}} - \log C_{H^+} - n \log a_{Nu} = \log \frac{k_2}{K_{SH_2^{2+}}} + m^{\ddagger} m^* X \quad (9)$$

where $m^{\ddagger}$ must be close to unity. To be able to plot the left-hand side of eq 9 vs X, the k_2 value should be previously determined if the equilibrium constant is already known. This equation was applied successfully to hydrolyses of benzoic acid derivatives and azopyridines.[32−35]

(iii) A-S_E2 Mechanism. Cox proposed a bimolecular pathway for the reaction scheme, involving rate-determining proton transfer to the monoprotonated substrate[20]

$$SH^+ + H^+ \xrightarrow{k_2} SH_2^{2+} \text{ slow} \quad (10)$$

$$SH_2^{2+} + H_2O \rightarrow P \text{ fast} \quad (11)$$

leading to the rate equation

$$\log k_{obs} - \log C_{H^+} = \log k_2 + m^{\ddagger} m^* X \quad (12)$$

(25) Cox, R. A.; Goldman, M. F.; Yates, K. *Can. J. Chem.* **1979**, *57*, 2960.
(26) Cox, R. A.; Yates, K. *J. Org. Chem.* **1986**, *51*, 3619.
(27) Ali, M.; Satchell, D. P. N. *J. Chem. Soc., Perkin Trans. 2* **1991**, 575.
(28) Satchell, D. P. N.; Wassef, W. N. *J. Chem. Soc Perkin Trans. 2* **1992**, 1855.
(29) Motie, R. E.; Satchell, D. P. N.; Wassef, W. N. *J. Chem. Soc., Perkin Trans. 2* **1993**, 1807.
(30) Alvarez, M. P.; Montequi, M. I. *An. Quim.* **1992**, *88*, 149.
(31) Montequi, M. I.; Alvarez, M. P. *An. Quim.* **1989**, *85*, 331.
(32) Cox, R. A.; Smith, C. R.; Yates, K. *Can. J. Chem.* **1979**, *57*, 2952.
(33) Cox, R. A.; Yates, K. *Can. J. Chem.* **1982**, *60*, 3061.
(34) Cox, R. A.; Onyido, I.; Buncel, E. *J. Am. Chem. Soc.* **1992**, *114*, 1358.

As mentioned above, the $m^{\ddagger}$ value is characteristic of the type of mechanism; in the case of an A-S_E2 scheme, $m^{\ddagger}$ should be less than 1. Equation 12 was applied to hydration of alkylesters and some phenylacetylene derivatives and hydrolyses of azocompounds and other substrates.[36−41]

The protonation acidity constant $pK_{SH_2^{2+}}$ needed for the proposal of this mechanism was calculated at high acidity by collecting and comparing the first spectral curves recorded in each kinetic run of a series of experiments similar to that of Figure 2, each performed at a different acidity. Up to about 6.5 M H_2SO_4 no significant spectral changes were observed; the changes in the first spectral curves, brought about by stepwise increase of medium acidity, enable the establishment of the protonation acidity range between 6.5 and 14.3 M H_2SO_4 using 10% v/v DMSO/H_2O. Figure 4a displays the spectral curves corresponding to dissociation of the doubly protonated form of the substrate; the appearance of a distorted isosbestic point reveals the presence of at least two species in equilibrium. By increasing the organic component in the solvent, the results became less accurate because reliable literature data of proton concentrations corresponding to H_2SO_4 concentration in mixed solvents are lacking.

The observed shifts in wavelengths can actually be attributed either to hydrolysis or to medium effects, or both. For a proper treatment of the medium effects we used the vector analysis method, already applied in amides[44] and pyrimidines[45] protonation, and the excess acidity method as well.[24] Figure 4b shows the reconstituted absorbance curves after application of vector analysis. The results were compared with those obtained using the excess acidity method, as stated by eq 7. The thermodynamic equation derived for equilibrium [2] is as follows

$$\log I - \log C_{H^+} = m^*X + pK_{SH_2^{2+}} \qquad (13)$$

where I is the ionization ratio calculated from the absorbances of the spectral curves, C_{H^+} is the proton concentration, and m^*, the slope parameter characteristic of the base, is 1.0 for primary aromatic amines,[46,47] 0.6 for amides,[44,46] 0.8 for carbocations,[47,48] etc. The three methods described above lead to very close results using the X values available for aqueous sulfuric acid; the average value is $pK_{SH_2^{2+}} = -5.8 \pm 0.1$ and $m^* = 0.94 \pm 0.03$. This constant corresponds to protonation of the $N_{(2)}$ site, the protonated form being responsible for further hydrolysis of the substrate (Scheme 2).

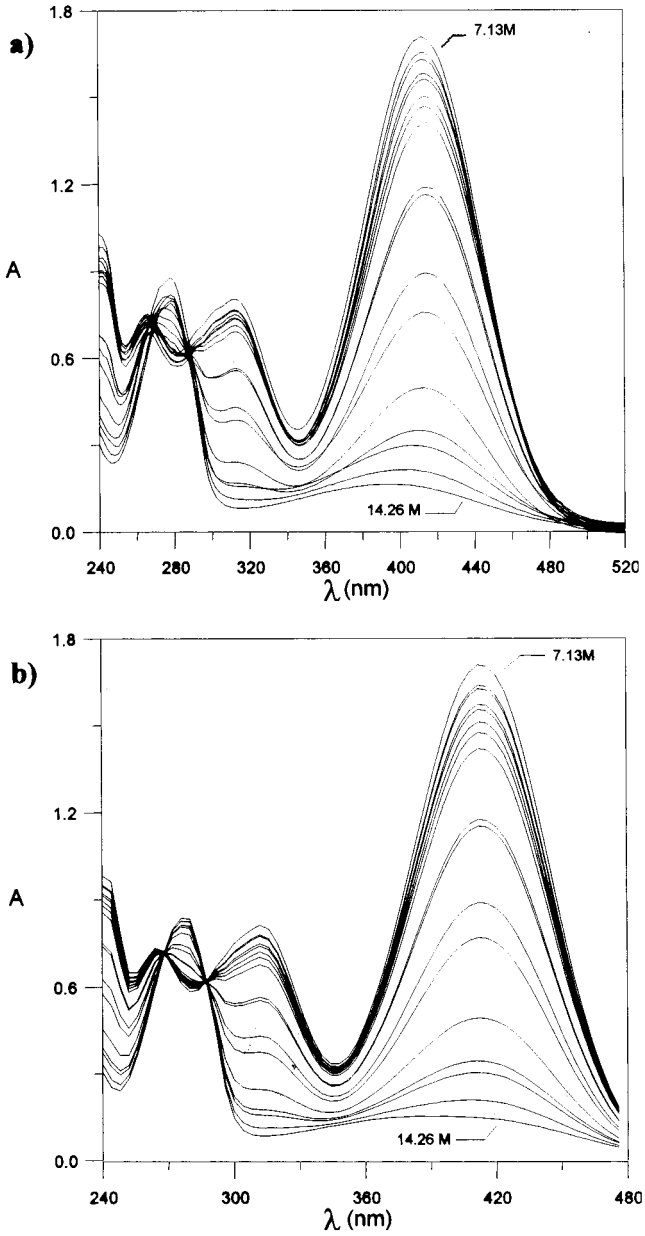

Figure 4. (a) Experimental absorbances corresponding to protonation $K_{SH_2^{2+}}$ of 2-acetylpyridinephenylhydrazone in 10% v/v DMSO/H_2O. (b) Reconstituted absorbances after application of vector analysis.

Once the thermodynamic parameters are known, it is feasible to carry out the kinetic calculations needed to determine the hydrolysis mechanisms.

(a) A-S_E2 Mechanism. The kinetic data of Figure 2 were analyzed with eqs 5, 9, and 12, corresponding to mechanisms A-l, A-2, and A-S_E2, respectively; within the first interval of low rate constants, ranging from 0.65 to ca. 5.84 M H_2SO_4, the reaction follows an A-S_E2 mechanism (Figure 5) (linear correlation coefficient, $r = 0.998$), according to which the rate-determining step should be the attack of a proton to SH^+; the value $m^{\ddagger} = 0.20$ also points to an A-S_E2 mechanism.[20] However, values of X are available in aqueous H_2SO_4 only,[10,24] this fact explaining why the best results correspond to the solvent with the highest water content. In this case, the rate

(35) Ghosh, K.K.; Rajput, S. K.; Krihnani, K. K. *J. Phys. Org. Chem.* **1992**, *5*, 39.
(36) Cox, R. A.; McAllister, M.; Roberts, K. A.; Stang, P. J.; Tidwell, T. T. *J. Org. Chem.* **1989**, *54*, 4899.
(37) Cox, R. A.; Grant, E.; Whitaker, T.; Tidwell, T. T. *Can. J. Chem.* **1990**, *68*, 1876.
(38) Cox, R. A. *J. Phys. Org. Chem.* **1991**, *4*, 233, **4**.
(39) Ali, M.; Satchell, D. P. N. *J. Chem. Soc., Perkin Trans 2* **1992**, 219.
(40) Joseph, V. B.; Satchell, D. P. N.; Satchell, R. S.; Wassef, W. N. *J. Chem. Soc., Perkin Trans. 2* **1992**, 339.
(41) Ali, M.; Satchell, D. P. N.; Le, V. T. *J. Chem. Soc., Perkin Trans. 2* **1993**, 917.
(42) Buncel, E.; Onyido, I. *Can. J. Chem.* **1986**, *64*, 2115.
(43) Onyido, I.; Opara, L. U. *J. Chem. Soc., Perkin Trans. 2* **1989**, 1817.
(44) García, B.; Casado, R. M.; Castillo, J.; Ibeas, S.; Domingo, P. L.; Leal, J. M. *J. Phys. Org. Chem.* **1993**, *6*, 101.
(45) García B.; Arcos J.; Domingo P. L.; Leal, J. M. *Anal. Lett.* **1991**, *24*, 391.
(46) Cox, R. A.; Yates, K. *Can. J. Chem.* **1984**, *62*, 2155.
(47) Cox, R. A.; Yates, K. *Can. J. Chem.* **1981**, *59*, 2116.
(48) García-Herbosa, G.; Muñoz, A.; Miguel, D.; García-Granda, S. *Organometallics* **1994**, *13*, 1775.

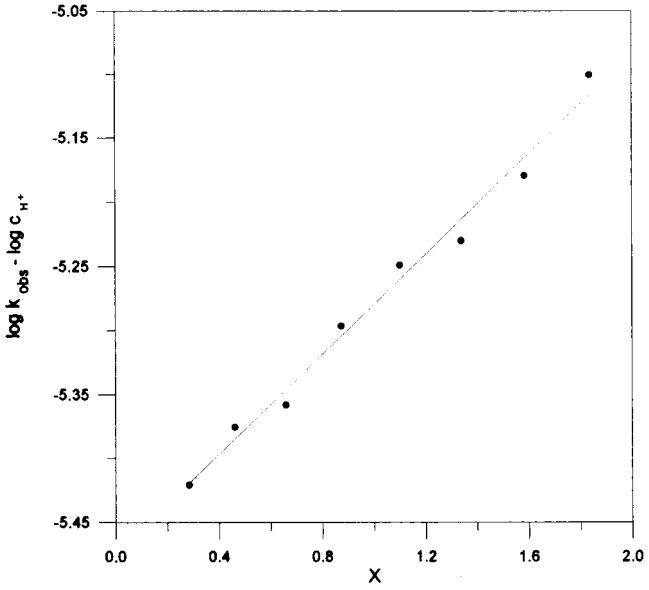

Figure 5. $k_{obs} - \log c_{H^+}$ vs X acidity plot in H_2SO_4 for an A-S_E2 scheme. $T = 25$ °C.

constant $k_2 = 3.35\ 10^{-6}\ M^{-1}\ s^{-1}$ was obtained for the rate-determining step. The protonation of a base normally is diffusion-controlled and, therefore, fast, with rate constants accessible by nonconventional techniques designed for fast reactions; however, among the wide variety of reactions that follow the A-S_E2 mechanism, there is in principle no upper limit in the k_2 value.[21,36−43]

This mechanism can be interpreted by Scheme 1. The attack of a second proton occurs on the "imine" $N_{(2)}$ nitrogen atom, the reaction site where hydrolysis occurs. The X-ray diagrams performed with the ligand[8,48] and other Pd complexes with this ligand confirm a planar structure and reveal proper bond distances and bond angles quite favorable for coordination by hydrogen bond to the two "pyridine" and "imine" N atoms.[49] The very stable syn conformer (II) of the diene group is the only structure existing at an acidity level below 0.6 M and is responsible for the substrate hydrolysis. The attack of a second proton on the $N_{(2)}$ atom of the hydrazone is difficult in the case of syn conformers; thus, above 0. 6 M H_2SO_4, the rotation of the σ (C−H) bond is feasible, giving rise to a balance between the syn (II) and anti (III) rotational conformers, the former being more stable. Since the number of anti conformers is very low and these species are involved in the protonation, it is reasonable to interpret the low k_2 rate constant as a value dependent on the concentration of anti conformers. Also the little effect of acidity on k_2 (Figure 3), points to the nonexistence of an acid−base balance within this acidity range, as can be inferred from the value $pK_{SH_2^{2+}} = -5.8$.

(b) A-2 Mechanism. Within the 6.4−11.6 M acidity range the fitting of kinetic data to eq 9 is fairly good (Figure 6, linear correlation coefficient, $r = 0.999$), the $m^{\ddagger} = 0.86$ value being reasonably close to unity, as required by the A-2 mechanism.[20] As in the above case, the protonation occurs on the nitrogen hydrazone group of the rotational anti conformer. However, above 6.4 M this step is fast, as confirmed by the acid−base balance established between the mono and diprotonated forms. The rate-determining step is the nucleophilic attack of a water molecule, with the rate constant $k_2 = 0.309\ M^{-1}\ s^{-1}$ obtained using the acidity function X.[22] The proposed mechanism is given in Scheme 2.

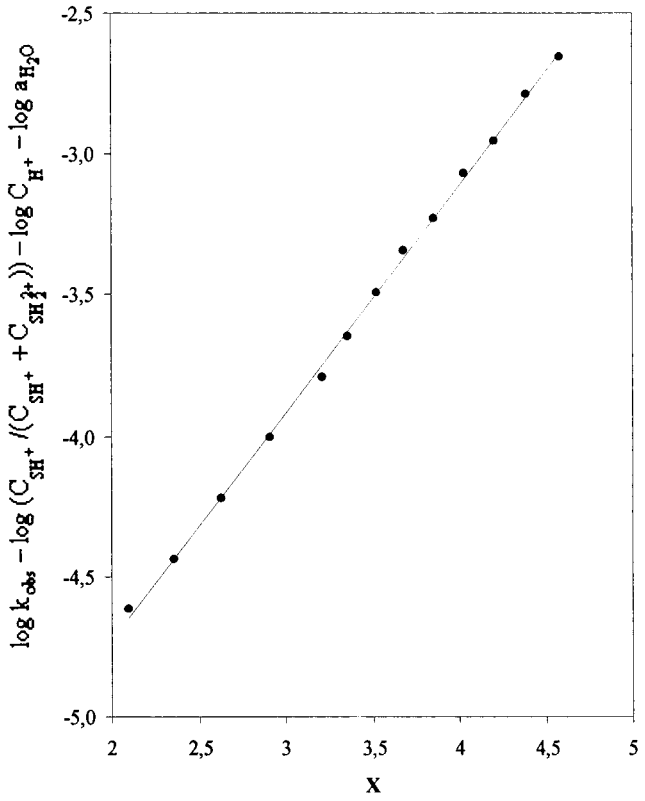

Figure 6. $\log k_{obs} - \log (C_{SH^+}/(C_{SH^+} + C_{SH_2^{2+}})) - \log C_{H^+} - \log a_{H_2O}$ vs X excess acidity plot for an A-2 scheme in H_2SO_4. $T = 25$ °C.

The rate constants increased with increasing solvent permittivity, this increase being greater at higher acidity. At constant acid concentration the change in reaction rate is in the following order: 10% DMSO/H_2O ($\epsilon = 78.5$) > 30% EtOH/H_2O ($\epsilon = 64.45$) > 50% EtOH/H_2O ($\epsilon = 53.44$). The rate constants of most reactions change with changes in solvent permittivity, including elementary reactions;[50] in the lower acidity range, A-S_E2 mechanism, the difference in the degree of solvation between the reagents and the transition state explains the solvent influence, since the transition state has a greater ionic character than the reagents.

The influence of solvent permittivity on the rate constant is much stronger in the high acidity range (A-2 mechanism). According to the transition-state theory, this feature might be attributed to the larger charge separation and, therefore, to the greater stability of the transition state compared to reagents. The noticeable solvation requirements of the hydrate make its stability to increase considerably as the solvent dielectric constant increases, this effect contributing to a decrease in activation energy. Several formulations have been developed to interpret the effect of solvent permittivity on the reaction rates of ion−ion, ion−dipole, and dipole−dipole in solution.[51−53]

(49) Scheiner, S. *Hydrogen Bonding. A theoretical Perspective*; OUP: New York, 1997.
(50) Funasaki, N.; Hada, S.; Neya, S. *J. Phys. Chem.* **1985**, *89*, 3046.
(51) Connors, K. A. *Chemical Kinetics. The study of Reaction Rates in Solution*; VCH: New York, 1990.
(52) Pilling, M. J.; Seakins, P. W. *Reaction Kinetics*; OUP: New York, 1995.
(53) Zuman P.; Patel, R. C. *Techniques in Organic Reactions Kinetics*; Wiley: New York, 1984.

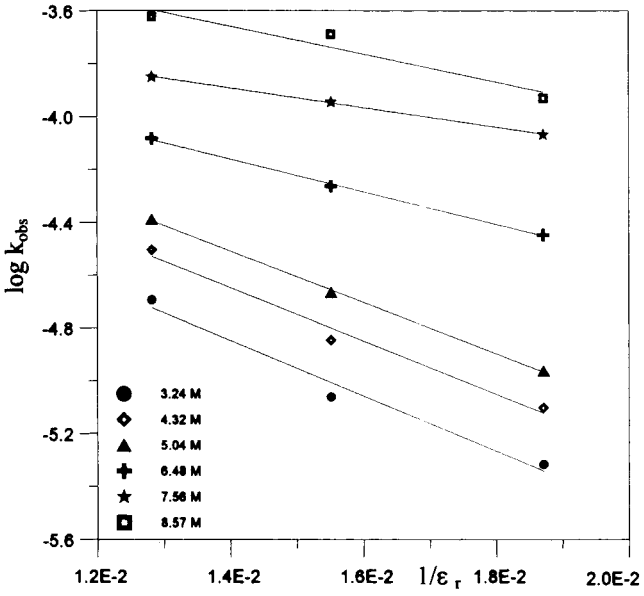

Figure 7. Plot showing the variation of log k_{obs} vs $1/\epsilon_r$ for the hydrolysis reaction at different acidity levels.

For reactions between two ions (which is the case in an A-S_E2 mechanism), the dependence of log k vs $1/\epsilon_r$ is as follows[11]

$$\ln k = \ln k_\infty - \frac{N z_A z_B e^2}{(4\pi\epsilon_o)\epsilon_r R T r_\ddagger} \qquad (14)$$

where k_∞ is the constant in the reference state of infinite dilution. In this work, the slope of the straight line should be negative, consistently with the obvious fact that the transition state is more polar than the positively charged reagents. In the case of ion−dipole interactions (A-2 mechanism), the following formulation was developed for the limit case of a zero approximation angle between the ion and the dipole:[51]

$$\ln k = \ln k_\infty - \frac{N Z_e^2}{(4\pi\epsilon_o)2\epsilon_r R T}\left(\frac{1}{r_{ion}} - \frac{1}{r_\ddagger}\right) \qquad (15)$$

The slope of the plot log k vs $1/\epsilon$ depends on the relative values of r_{ion} and $r_\ddagger$ the radius of the transition state. Figure 7 plots the values log k vs $1/\epsilon_r$ at different acid concentrations. In this figure, the eqs 14 and 15 are written out and a clear parallelism can be seen mainly in the acidity range corresponding to the A-S_E2 mechanism; the negative slope is consistent with a transition state positively charged and more polar than the reagent, in accordance with the proposed mechanism; obviously, the r_{ion} radius is smaller than $r_\ddagger$, consistent with the proposed mechanism. The somewhat smaller parallelism observed in the A-2 range can be explained by the lack of acidity functions in the media under study, which causes greater effects when the acid concentration is increased.

Acknowledgment. The finantial support by the spanish DGESIC, project PM97-0153, and Junta de Castilla y León, project BU08/97, are gratefully acknowledged.

JO000085M